ELSEVIER

International Journal of Fatigue 21 (1999) 1033–1049

International Journal of Fatigue

www.elsevier.com/locate/ijfatigue

Fatigue life prediction of fiber reinforced concrete under flexural load

Jun Zhang [a,*], Henrik Stang [b], Victor C. Li [a]

[a] *Advanced Civil Engineering Materials Research Laboratory, Department of Civil and Environmental Engineering, University of Michigan, Ann Arbor, MI 48109, USA*

[b] *Department of Structural Engineering and Materials, Technical University of Denmark, DK2800, Lyngby, Denmark*

Received 8 February 1999; received in revised form 20 June 1999; accepted 10 July 1999

Abstract

This paper presents a semi-analytical method to predict fatigue behavior in flexure of fiber reinforced concrete (FRC) based on the equilibrium of force in the critical cracked section. The model relies on the cyclic bridging law, the so-called stress–crack width relationship under cyclic tensile load as the fundamental constitutive relationship in tension. The numerical results in terms of fatigue crack length and crack mouth opening displacement as a function of load cycles are obtained for given maximum and minimum flexure load levels. Good correlation between experiments and the model predictions is found. Furthermore, the minimum load effect on the fatigue life of beams under bending load, which has been studied experimentally in the past, is simulated and a mechanism-based explanation is provided in theory. This basic analysis leads to the conclusion that the fatigue performance in flexure of FRC materials is strongly influenced by the cyclic stress–crack width relationship within the fracture zone. The optimum fatigue behavior of FRC structures in bending can be achieved by optimising the bond properties of aggregate–matrix and fiber–matrix interfaces.

Keywords: Crack bridging; Fatigue crack growth; Fiber reinforced concrete; Flexural loading; Model

1. Introduction

The incorporation of steel or other fibers in concrete has been found to improve several of its properties, primarily cracking resistance, impact and wear resistance and ductility. For this reason fiber reinforced concrete (FRC) is now being used in increasing amounts in structures such as airport pavements, highway overlays, bridge decks and machine foundations. However, most of these structural elements are loaded in cyclic loading. For example, the concrete overlays for highway or bridge decks are expected to resist millions of cycles of repeated axle loads from passing traffic during their service life. Airport pavements are subjected to a smaller number of repeated loadings during their designed life ranging from about several thousand to several hundred thousand cycles of repeated loading. Concrete structures supporting dynamic machines are also subjected to hundreds of millions of load cycles involving complicated stress states. The fatigue performance of these structures has to be considered by researchers and designers. First, the cyclic load may cause structural fatigue failure. Second, the effects of repeated loading on the characteristics of materials (static strength, stiffness, toughness, durability, etc.) may be significant under service loading, even if the load does not cause a fatigue failure.

As it is a relatively new material, the history of investigation on the fatigue of FRC is not long. Experimental evaluations of this behavior have been carried out in recent years [1–6]. Fatigue life prediction and the design of FRC structures can so far only be performed through an empirical approach. This approach requires time-consuming test data collection and processing for a broad range of design cases which, in principle, is not applicable to other design cases. Therefore, a mechanism-based fatigue model that is capable of both predicting the fatigue life for a given FRC structure and designing an FRC material for a given fatigue life has to be set up for the above reasons [7]. In order to do so, the mechanism of fatigue crack propagation in FRC material has to be understood first.

* Corresponding author.

0142-1123/99/$ - see front matter
PII: S0142-1123(99)00093-6

Normally, it can be said that fatigue is a process of progressive, permanent internal structural changes occurring in a material subjected to repetitive stress. The progressive fatigue damage on material constituents is responsible for fatigue life of a material. For FRC, the material phases can broadly be classified as matrix (cement paste and aggregates), fibers, as well as the interfaces of fiber–matrix and aggregate–hydrated cement paste. The fatigue loading causes these physical phases to undergo microscopic changes, such as opening and growth of bond cracks, which exist at the interface between coarse aggregate and hydrated cement paste even prior to the application of load [8], reversed movement of fiber along the interface, fiber surface abrasion and damage of interface in repeated sliding processes. These microscopical changes, in turn, cause some detrimental changes in macroscopic material properties. Typically, the aggregate bridging force as well as the fiber bridging force decreases with the number of cycles, due to interfacial damage [9] or fiber breakage due to surface abrasion [10]. So it can be said that the damage on interfaces of fiber–matrix and aggregate–matrix, which are generally the weakest phase in concrete and FRCs, as well as on soft polymer fibers is responsible for fatigue crack initiation and growth in concrete and FRCs. On the other hand, the fatigue life of concrete and FRC structures is controlled by fatigue crack growth behavior.

The fatigue crack growth process in concrete or FRC materials can be broadly divided into two stages: the crack initiation period and the development period. Now considering a simply supported rectangular beam loaded in bending fatigue load with a constant amplitude between the maximum and minimum moment, $M_{\max}$ and $M_{\min}$. When $M_{\max}<M_{fc}$, where M_{fc} is the first crack moment, the fatigue life of the beam can be given by:

$$N_t=N_{ci}+N_{cg} \tag{1}$$

When $M_{\max}\geq M_{fc}$, the fatigue life is:

$$N_t=N_{cg} \tag{2}$$

where N_t is the total fatigue life, N_{ci} and N_{cg} are the fatigue life component for the crack initiation and growth, respectively, see Fig. 1. The first term, N_{ci}, is dependent on the microcracking in material, which is highly influenced by the microstructure of concrete matrix, such as the water/cement ratio, aggregate properties as well as pore structure, size distribution and content. The second term, N_{cg}, is strongly dependent on the bridging performance within the fracture zone under fatigue loading.

This paper focuses on the fatigue life prediction on N_{cg}, i.e. the case of maximum load, $M_{\max}$, is larger than the first crack load, M_{fc}. Based on the above discussions, some basic assumptions for fatigue modelling on N_{cg} can be stated:

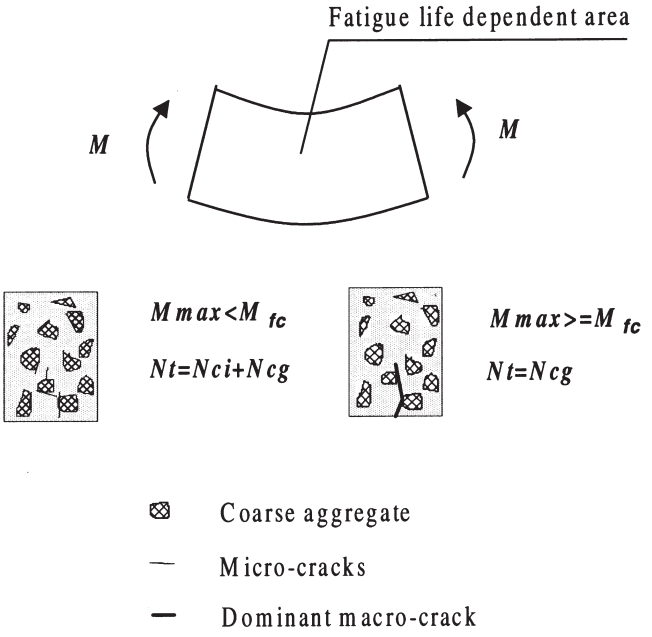

Fig. 1. Fatigue life components in bending.

1. After a dominant fatigue crack is created, the bridging behavior within the fracture zone is governing the rate of fatigue crack advancement.
2. The stress at the crack tip remains constant and is equal to the material tensile strength.
3. Material properties outside the fracture zone are unchanged during fatigue loading.

It is further assumed that concrete and FRC materials essentially show a linear response in tension up to peak load. After peak one discrete crack is formed, and the discrete crack formation is described by the crack bridging law (or stress–crack width relationship) under both monotonic and cyclic loading. Thus, the following material parameters are fundamental in the constitutive relationships of concrete and FRC in fatigue tension: the Young's modulus E, the tensile strength σ_t and the cyclic stress–crack width (σ–w,N) relationship. In compression the behavior of concrete and FRC materials is assumed to be linear elastic and the Young's modulus in compression is the same as in tension.

With the above assumptions, a semi-analytical method for predicting fatigue behavior of unreinforced concrete and FRC beams under bending load is developed in the present work. In this model, the cyclic bridging law (or cyclic stress–crack width relationship) is incorporated in integration form, which can easily be replaced by the other bridging models for different kinds of FRC materials with different fiber types, volume concentrations and matrix properties. In this paper, a quart-linear monotonic stress–crack width model, based on the uniaxial tensile test results, applied to plain concrete and two types of concrete reinforced with straight and

hooked steel fiber, respectively, is adopted. The complete theoretical curves, in terms of fatigue crack length or crack mouth opening displacement (CMOD) with number of cycles diagrams, as well as the classical S–N curves are obtained and compared with the experimental results. The results are discussed and conclusions are draw at end of the paper.

2. Bridging model of concrete and FRCS under fatigue tension

In order to determine the cyclic stress–crack width relationship experimentally, deformation-controlled fatigue tensile tests were conducted on notched specimens with a thickness of 50 mm, width 60 mm and height 55 mm. To eliminate the pre-stressing inevitably introduced in the specimens when using conventional grips, for improved alignment, and for maximum stiffness, a special specimen fixture developed by Stang and Aarre [11] was used. The fixture consists of a permanent part and an interchangeable steel block, which is fixed to the permanent part through four bolts. The specimen is glued to the blocks. The glued surfaces of the interchangeable steel blocks and the specimen are sand-blasted before gluing to enhance the bond between steel and specimen. By having a large number of such steel blocks, multiple specimens can be tested continuously, as it is not necessary to clean the steel blocks after each test. As soft connections between the interchangeable steel blocks and the machine are eliminated, the set-up takes full advantage of the stiffness of the machine frame. It should thus be ensured that the rotational stiffness of the test set-up is large compared to the rotational stiffness of the concrete specimen. A fast curing polymer which attains 90% of its maximum strength in about 4 min was used. The deformation was measured using two standard Instron extensometers (type 2620-602) with 12.5 mm gauge length mounted across each of the two 9 mm deep and 3 mm wide notches. The tests were performed in a 250 kN load capacity 8500 Instron dynamic testing machine equipped for closed-loop testing. The experimental set-up is shown in Fig. 2.

The uniaxial fatigue tensile test was conducted under displacement control with constant amplitude between maximum and minimum pre-crack widths (w_{max} and w_{min}). The minimum crack width value was obtained by a single loading–unloading tensile test at which the bridging load is equal to zero on the unloading branch. The fatigue test commenced with a ramp to the minimum crack value at a rate of 0.01 mm/s followed by a sine waveform fatigue loading in deformation control. In order to control the accuracy of the maximum crack width value, different load frequencies of 0.25 Hz in the first two cycles and 3.5 Hz for the rest of cycles were adopted. This fatigue load procedure is shown in Fig. 3.

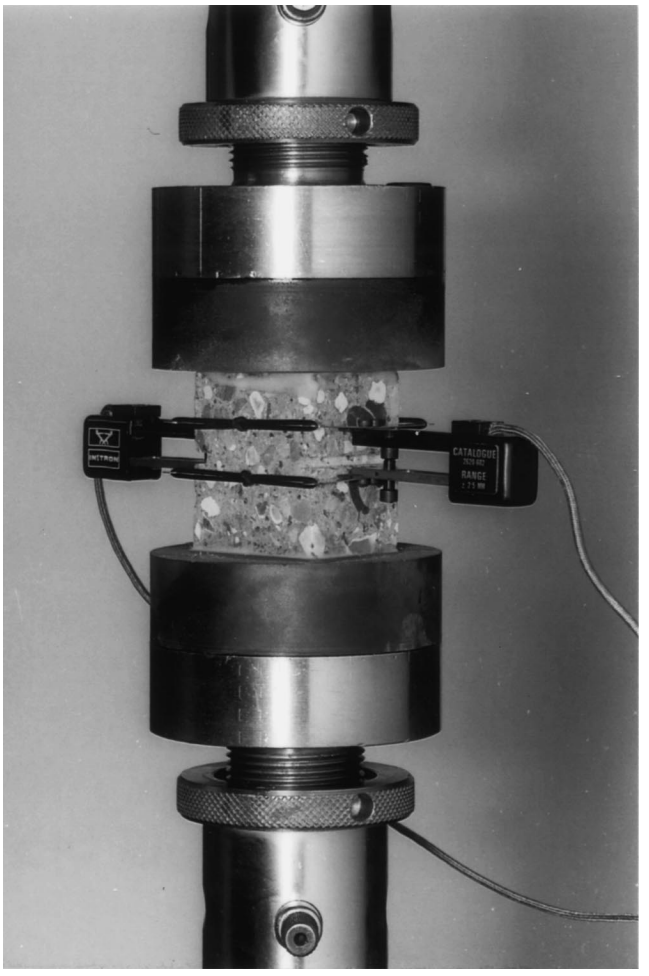

Fig. 2. Schematic view of the test set-up for fatigue tension.

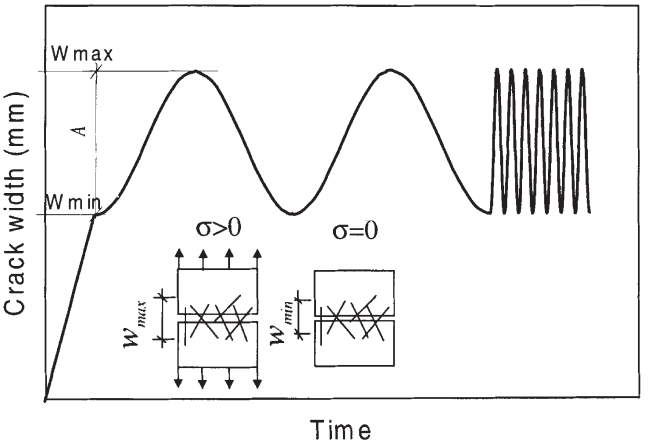

Fig. 3. Deformation-time diagram in fatigue test.

Technical details on the testing procedure can be found elsewhere [12].

In the present investigation, two types of commercially available steel fibers, smooth and hooked-end, with circular cross-section, 0.4 and 0.5 mm in diameter, 25 and 30 mm in length, respectively, were used separ-

Table 1
Mix proportions of steel fiber concrete

Component	Amount (kg/m^3)
Cement	500
Sand (maximum particle size 4 mm)	810
Gravel (maximum particle size 8 mm)	810
Superplasticizer (66% water content)	3.25
Water	237.5
Smooth or hooked steel fibers	78.4
Fiber volume content (%) V_f	1

ately in the same matrix. A rapid hardening cement, natural sand and stone with maximum particle size of 4 and 8 mm, respectively, were used. The concrete mix is shown in Table 1. All pre-notched specimens were cut out of beams of 50 mm width, 100 mm depth and 350 mm length. Details of specimen preparation can be found in Zhang et al. [12].

Experimental results of uniaxial fatigue tension tests on pre-cracked plain concrete and FRCs show that the bridging stress decreases with the number of load cycles for the same crack openings. Typical test results on both smooth steel fiber concrete (SSFRC) and hooked steel fiber concrete (HSFRC), are shown in Fig. 4, where the maximum bridging stress corresponding to the maximum crack width is normalised to the stress level at first cycle. The experimental investigation and theoretical analysis show that the cyclic bridging law of FRCs is quite complicated and can be influenced by many parameters, including material constituents as well as loading conditions, such as maximum and minimum crack width levels [12,13]. The material parameter-based micromechanical model of cyclic bridging law, however, may be too complicated to be used as a fundamental constitutive relationship directly in structural numerical analyses. A more simple and effective way to carry out the numerical simulations is to use a mathematical fit that is based on the experimental results and theoretical analysis as the input of cyclic bridging law. This process, in principle, will not affect the applications of the theoretical model in fatigue optimisation and the design of new types of FRC materials based on the micromechanical parameters of the material; however, the predictions are limited to the range in which the fitting is done. In the present work, a mathematical fit on the cyclic crack bridging law is applied in the fatigue performance prediction.

From a large number of experimental data on uniaxial fatigue tension tests on pre-cracked specimens [12], the cyclic crack bridging law at the maximum crack width level, w_{max}, can be fitted by a multi-linear model as a function of the logarithm of the number of cycles. The multi-linear model is given by:

$$\frac{\sigma_N}{\sigma_1}=1-f(w_{max},w_{min})\log(N)$$
$$=1-\varphi g(w_{max},w_{min0})\log(N) \quad (3)$$

where σ_N, σ_1 are the stresses at the maximum crack width, w_{max}, after N cycles and the first cycle, respectively. The σ_1 is simulated by a quart-linear model based on the directly measured stress–crack width (σ–w) data [14], that is:

$$\frac{\sigma_1}{\sigma_t}=a_i+b_i w_{max}(i=1\ldots4) \quad (4)$$

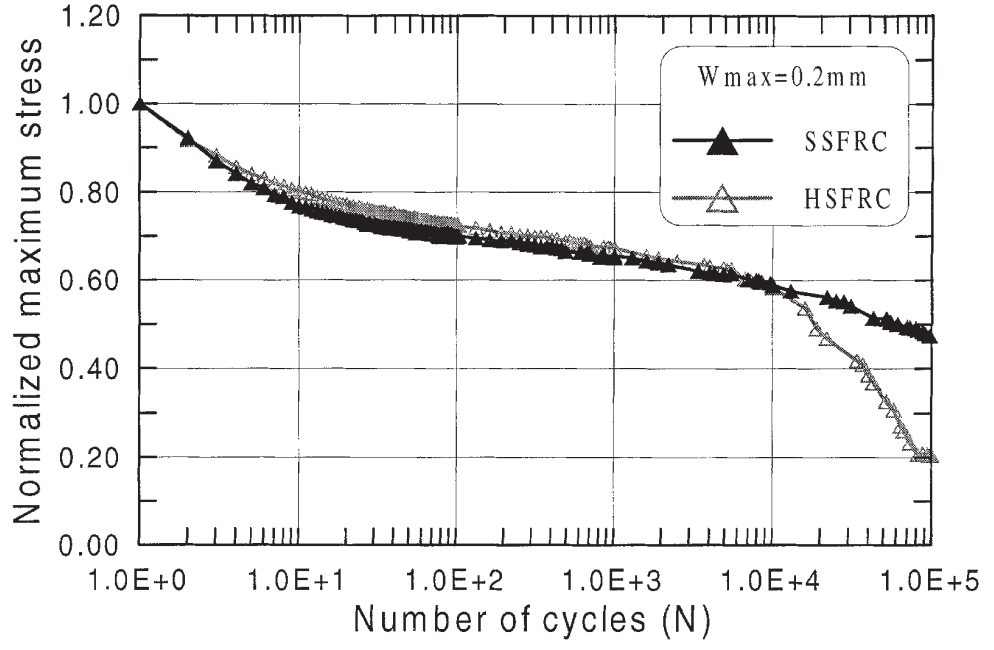

Fig. 4. Typical test results of bridging stress vs. number of cycles.

Here σ_t is tensile strength of material, and the parameters a_i and b_i are given in Table 2. The function $f(w_{max},w_{min})$ is a function of maximum and minimum crack width values, w_{max} and w_{min}, which describes the effect of the maximum and minimum crack opening on the rate of bridging degradation. This function can further be rewritten as a product of a parameter φ and a function of only the maximum crack width, w_{max}. The parameter $\varphi(\varphi\in[0,1])$ reflects the influence of minimum crack width, w_{min}, on the bridging degradation. φ is defined as:

$$\varphi=\frac{w_{max}-w_{min}}{w_{max}-w_{min0}} \tag{5}$$

where w_{min0} is the minimum crack width as the bridging force equals to zero. From the definition of φ, it can be seen that as w_{min} goes up, φ will go down, that means the rate of bridging degradation will also go down. These are consistent with the theoretical and experimental results [14]. The minimum degradation will occur as w_{min} is equal to w_{max}, (φ=0), and the maximum degradation will happen at w_{min} equal to w_{min0}, (φ=1).

The detailed expressions of Eq. (3) for different kinds of concrete are given in Appendix A. Figures 5 to 7 show the fit-based cyclic bridging law for different kinds of concrete, including plain concrete, steel fiber concrete, SSFRC and HSFRC. For the FRCs, the experimental results in the case of φ equal to one are presented together with the model predictions. The figures show the bridging degradation at different maximum crack width after undergoing a certain number of cycles. As the maximum and minimum crack widths vary with the number of cycles, such as that for a beam under fatigue bending, the parameters w_{max} and w_{min} used in Eq. (3) will be replaced by the representative values, i.e. the average of all the loading history.

3. Prediction of fatigue crack growth in concrete and FRC beam under bending load

In recent years, a number of fictitious crack [15] based analytical models for predicting the structural behavior of concrete and FRC beams under bending load have been developed. Ulfkjær et al. [16] developed an analytical model of a plain concrete beam in bending based on plastic hinge analysis, which assumes the development of a fictitious crack in an elastic layer with a thickness proportional to the beam depth. A linear tension softening relationship is assumed. Pedersen [17] developed a similar model for plain as well as FRC structures, beams and pipes, in which a more accurate softening law, a power function proposed by Stang and Aarre [11], is adopted. Maalej and Li [18] developed an analytical model of a FRC beam in bending based on the equilibrium of force in the critical cracked section. Here the authors adopt the analytical softening relationships presented by Maalej et al. [19] and Li [20]. Recent theoretical studies show that the bridging law for smaller crack widths, typically less than 0.1 mm, can strongly affect the structural behavior of beams in bending under monotonic and cyclic loads [21]. In this paper, an analytical bending model based on the equilibrium of force in the critical cracked section with a multi-linear softening relationship [14] for fatigue analysis will be developed.

Consider a short segment of a simple supported rectangular beam with width B, depth h, and span L that is subjected to an external bending moment M. The behavior of the beam is assumed to be elastic until the maximum principle tensile stress reaches the tensile strength of the material. After that it is assumed that a single crack is formed with a maximum tensile strength at the crack tip. The moment corresponding to the initiation of the fictitious crack is the so-called first crack moment, M_{fc}, or first crack load, P_{fc}, when the moment is transformed into load. Thus, the failure process of the beam can be divided into two stages: (1) a linear elastic stage; and (2) a fictitious crack developing stage. The assumed stress distribution in the second stage is shown in Fig. 8.

In the first stage, according to classical elastic theory, we have:

$$M_{fc}=\frac{Bh^2}{6}\sigma_t \tag{6}$$

Table 2
Material parameters of three types of concrete

Material parameters	SSFRC	w (mm)	HSFRC	w (mm)	PC	w (mm)
E (GPa)	35	–	32	–	30	–
σ_t (MPa)	5.42	–	5.30	–	5.20	–
σ_c (MPa)	55.2	–	55.0	–	53.22	–
a_1, b_1 (1/mm)	1,−9.96	0–0.03	1,−8.73	0–0.04	1,−33.48	0–0.017
a_2, b_2 (1/mm)	0.685,0.526	0.03–0.10	0.632,0.472	0.04–0.18	0.569,−8.12	0.017–0.044
a_3, b_3 (1/mm)	0.883,−1.45	0.10–0.38	0.8,−0.463	0.18−0.75	0.321,−2.49	0.044−0.081
a_4, b_4 (1/mm)	0.374,−0.11	0.38–2	0.532,−0.106	0.75–2	0.187,−0.84	0.081–0.2

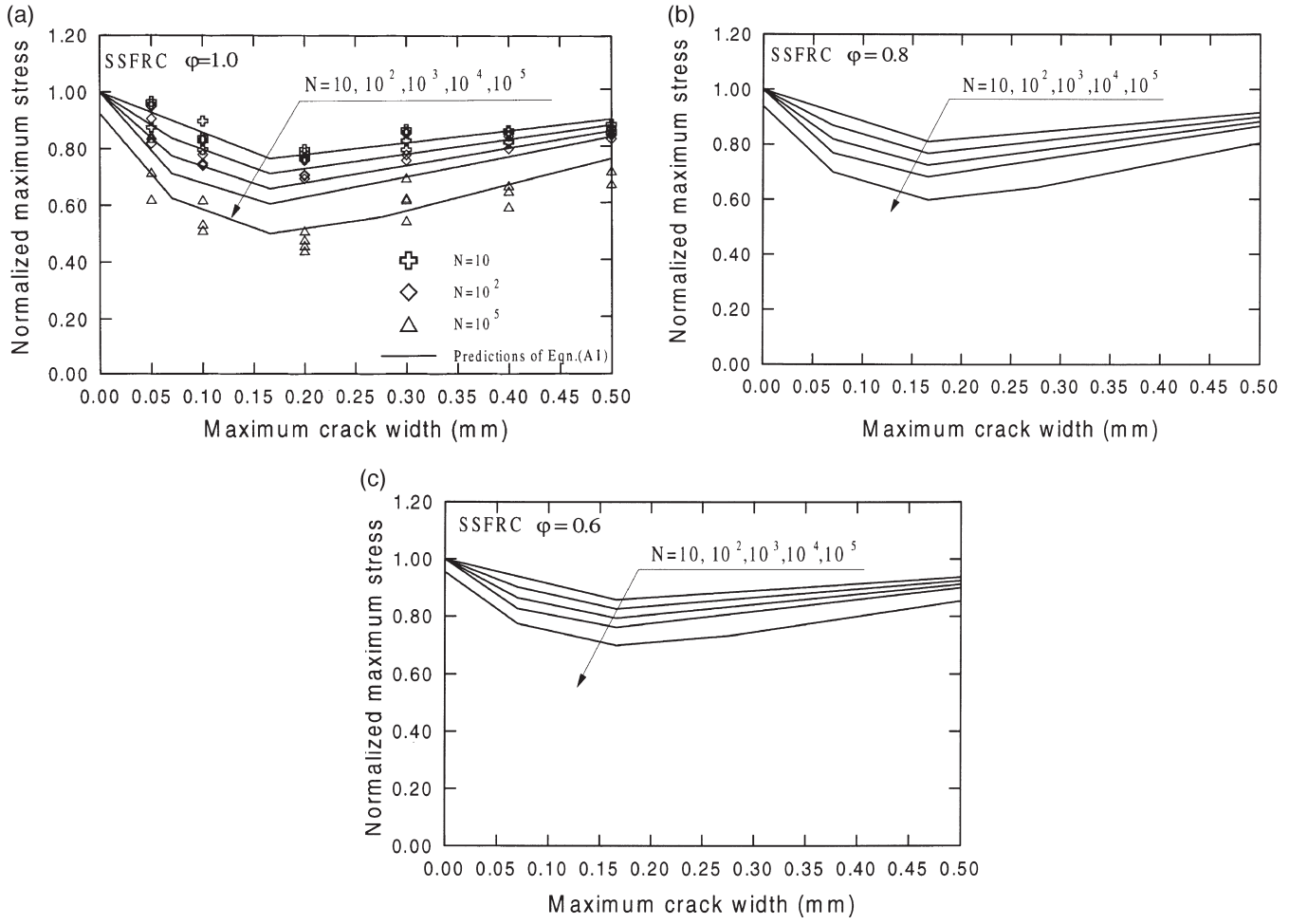

Fig. 5. Model predictions on crack bridging degradation of SSFRC, showing the effect of φ.

where σ_t is the tensile strength of materials.

In the second stage, the crack length αh, $\alpha \in [0,1]$, CMOD, δ and external moment M can be related through the analysis below. First we assume that the crack has a linear crack opening profile, then:

$$w=\delta\left(1-\frac{x}{\alpha h}\right) \tag{7}$$

where w is crack width at location x, see Fig. 8. Next, from the equilibrium conditions, we have:

$$\int_0^{\alpha h}\sigma_I(x)dx+\int_{\alpha h}^{h}\sigma_{II}(x)dx=0 \tag{8}$$

$$\int_0^{\alpha h}\alpha_I(x)(h-x)Bdx+\int_{\alpha h}^{h}\sigma_{II}(x)(h-x)Bdx=M \tag{9}$$

where $M=PL/4$ for the three-point bending case (P is external load) and $\sigma_I(x)$, $\sigma_{II}(x)$ are the normal stress function in the cracked and uncracked parts, respectively. $\sigma_I(x)$ can be related with αh and δ through the stress–crack width relationship together with Eq. (7) as:

$$\sigma_I(x)=\sigma(w)=\sigma\left(\delta\left(1-\frac{x}{\alpha h}\right)\right) \tag{10}$$

From the assumed stress distribution at the uncracked part, $\sigma_{II}(x)$ can be related to αh, βh and δ by:

$$\sigma_{II}(x)=\sigma_t\left(1-\frac{x-\alpha h}{\beta h-\alpha h}\right) \tag{11}$$

where βh is the depth of tensile zone, $\beta \in [0,1]$. In order to obtain the complete solution of external load and CMOD for a given crack length, another relationship between them is necessary. According to the principle of superposition, the CMOD under bending load can be decomposed as:

$$\delta=\delta_M+\delta_{\sigma I(x)} \tag{12}$$

where δ_M and $\delta_{\sigma I(x)}$ are the CMOD component caused by external moment M and bridging stress $\sigma_I(x)$, respect-

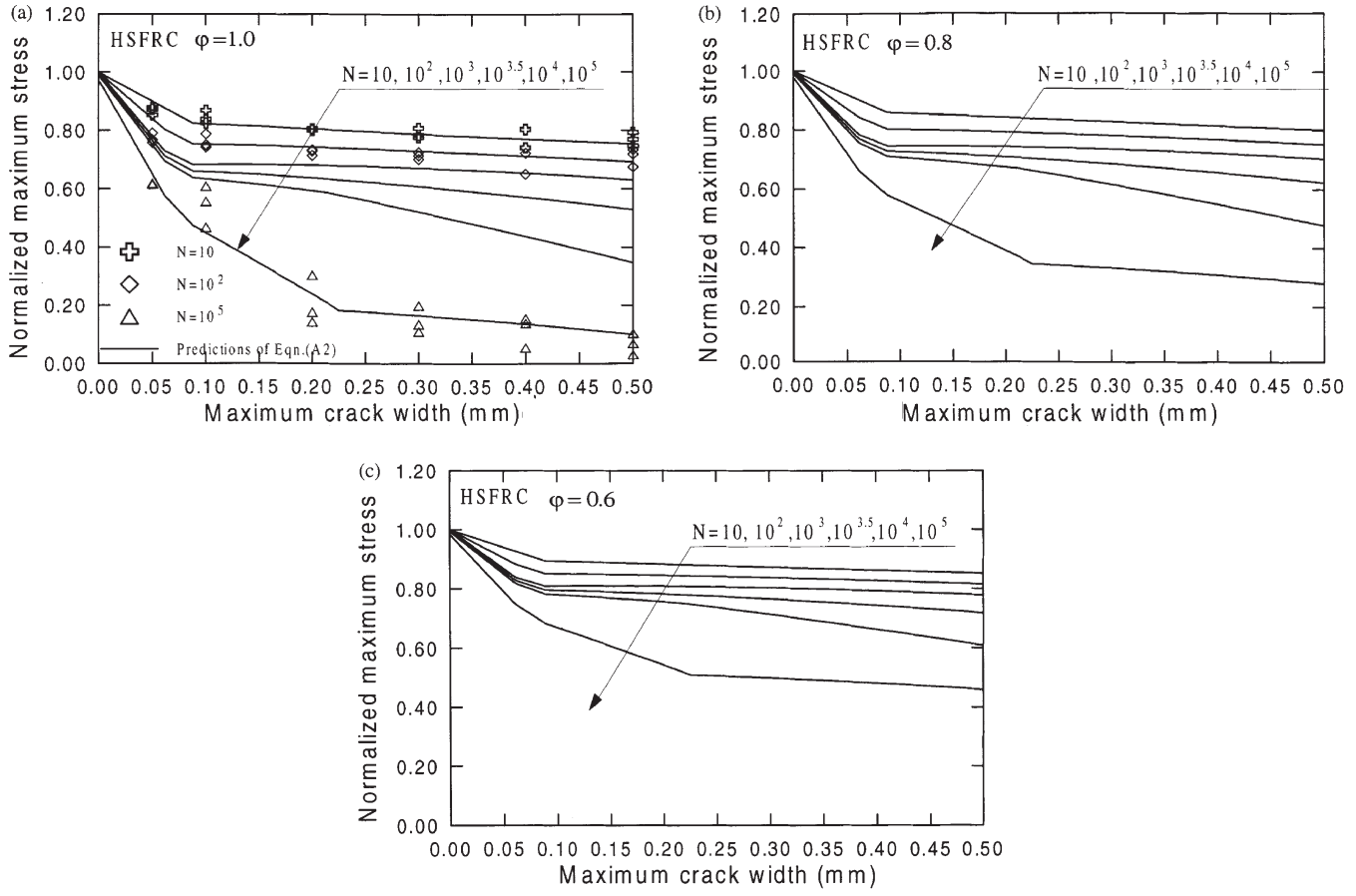

Fig. 6. Model predictions on crack bridging degradation of HSFRC showing the effect of φ. (a) φ=1.0; (b) φ=0.8 and (c) φ=0.6.

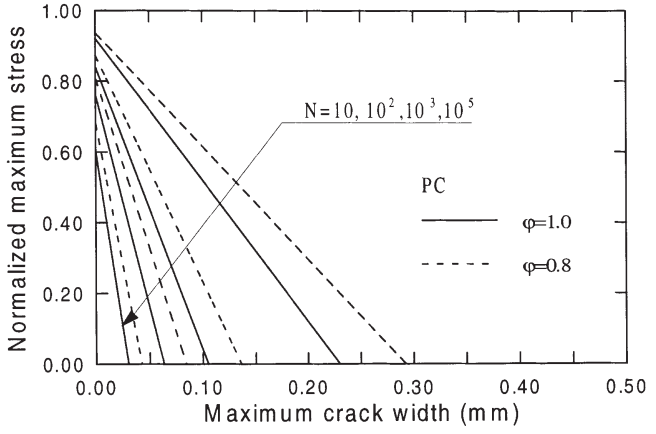

Fig. 7. Model predictions on crack bridging degradation of plain concrete showing the effect of φ.

ively. $\delta_{\sigma I(x)}$ can be obtained through simplifying $\sigma_I(x)$ as a cracked beam with crack length αh and subjected to moment M' and axial stress σ'. Then:

$$\delta_{\sigma I(x)}=\delta_{M'}+\delta_{\sigma'} \tag{13}$$

here M' and σ' are given by:

$$M'=\int_0^{\alpha h} B\sigma_I(x)\left(\frac{h}{2}-x\right)dx \tag{14}$$

$$\sigma'=\frac{1}{h}\int_0^{\alpha h}\sigma_I(x)dx \tag{15}$$

According to Tada [22], the total CMOD can be expressed as:

$$\delta=\frac{24\alpha}{BhE}[MV_1(\alpha)-M'V_2(\alpha)]-\frac{4\sigma'\alpha h}{E}V_3(\alpha) \tag{16}$$

where, under three-point bending load,

$$V_1(\alpha)=0.33-1.42\alpha+3.87\alpha^2-2.04\alpha^3+\frac{0.66}{(1-\alpha)^2}$$

$$V_2(\alpha)=0.8-1.7\alpha+2.4\alpha^2+\frac{0.66}{(1-\alpha)^2}$$

$$V_3(\alpha)=\frac{1.46+3.42\left(1-\cos\frac{\pi\alpha}{2}\right)}{\left(\cos\frac{\pi\alpha}{2}\right)^2}$$

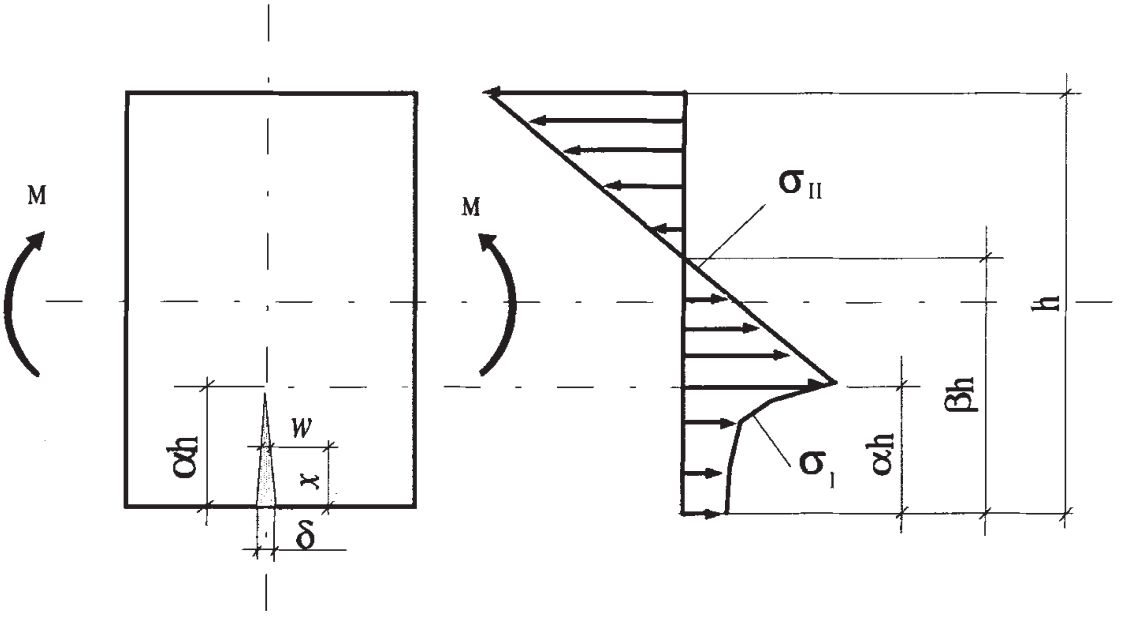

Fig. 8. Distribution of normal stress in the critical cracked section.

Here $V_1(\alpha)$ is slightly changed from Tada's function after comparing with the authors' finite element implementation [14].

According to the basic assumptions given in Section 1, as a first approximation, the fatigue analysis can be performed by replacing the bridging stress in the fracture zone, $\sigma_I(x)$ with the cycle dependent models given by Eq. (3). The determination of fatigue crack length and crack mouth opening, corresponding to certain cycles for a given fatigue loading procedure, is performed according to the following algorithm.

For a given maximum and minimum load level M_{max}, M_{min} (here the case of $M_{max}>M_{fc}$ is considered only), in the first cycle, the crack length and crack mouth opening are determined by solving the nonlinear Equations (8), (9) and (16) through a simple bisection iteration scheme. The bridging law without stress degradation (N=1) will be used as the input for $\sigma_I(x)$, and the numerical integration method is used. In the second cycle (N=2), since the fatigue crack undergoes a closing and opening procedure, bridging degradation will occur in the fracture zone. The load capacity M cannot reach M_{max} with the already formed crack area when this crack opens to the previous maximum width. Therefore, a new crack area is needed in order to reach the maximum load level. The bridging laws with N=2 and N=1 will be used in the old fracture zone and the newly developed fracture zone, respectively. Solving Equations (8), (9) and (16) again, the newly developed crack length Δa_2 and crack mouth opening δ can be obtained. Through similar calculations, we can get all the newly developed crack lengths Δa_3, Δa_4, Δa_5 and corresponding crack mouth openings at cycles 3, 4, 5…. This procedure will be continued until the load capacity starts to drop with the increasing crack length. According to this procedure, for the Nth load cycle, the fracture zone will be divided into N sections with different fatigue histories, ranging from 1 to N cycles. In order to speed up the calculation procedure, increments with more than 1 cycle can be used, normally five to 10 or 20 cycles. This depends on the load level, fatigue crack growth rate and the required accuracy. In this case, a linear interpolation of crack length in one increment has been used.

4. Numerical results, experimental verification and discussions

4.1. Fatigue tests

In order to verify the model, three-point bending fatigue tests on two types of steel fiber concrete beams, with smooth and hooked steel fibers, respectively, are conducted. The concrete proportions of these two FRCs are the same as those used in fatigue tension tests. The size of the beam is 420×100×100 mm and the span is 400 mm. One-stage constant amplitude fatigue loading between maximum and minimum load levels, M_{max}, and M_{min}, where M_{min} is equal to zero, is adapted. The tests are carried out in load control using a sinusoidal waveform with a frequency of 4.5 Hz. The deflection is measured carefully during testing using a reference beam attached to the top of the beam by three steel blocks glued to the beam surface. Two standard Instron extensometers (type 2620-602) with 12.5 mm gauge length are used for measuring the deflection. The crack mouth opening displacement is measured by an extensometer mounted on the middle section of the tensile side of

beam with 50 mm gauge length. The crack mouth opening displacement is equal to the measured deformation Δl minus the elastic deformation inside the gauge length. By assuming that the stress in the gauge length is equal to the stress transferred by the crack, the CMOD at the maximum load level can be calculated by:

$$\delta=\frac{\Delta\bar{l}-a_{iN}}{\xi+b_{iN}} \tag{17}$$

where $\Delta\bar{l}=\Delta l/\Delta l_t$, $\xi=1/\Delta l_t$, $\Delta l_t=\sigma_t\ l/E$, l is the gauge length. $a_{iN}=a_i[d+e\log(N)]$ and $c_{iN}=b_i[d+e\log(N)]$, a_i , b_i are given by the stress–crack width model given by Eq. (4). d, e can be determined from Equations (A1) and (A2), given in Appendix A. N is the number of cycles. The experimental set-up used for FRC beams in three-point bending is shown in Fig. 9. All of the tests are carried out in a a 250 KN capacity, 8500 Instron dynamic testing machine.

4.2. S–N curves

Fatigue strength is commonly defined as a fraction of the static strength that can be supported repeatedly for a given number of cycles. It can be represented by stress–fatigue life curves, normally referred to as S–N curves. In the case of fatigue in bending, S refers to the flexural stress according to classical elastic theory.

As an example, a specific fatigue loading procedure with $M_{\min}$ equal to zero that fits the condition of fatigue tension and bending tests is assumed in the first numerical calculation. The effect of minimum load level on S–N diagrams will be presented in the next section. The geometry of the specimen is the same as that used in the fatigue bending tests, and the cyclic bridging laws for different types of concrete described in Section 2 are used in the analysis. The related material parameters are listed in Table 2. In order to compare the results between monotonic loading and fatigue loading, the monotonic bending behavior is simulated first in terms of the load CMOD relationship. Fig. 10 shows the monotonic flexural stress–CMOD curves of plain concrete and the two types of steel fiber reinforced concrete (SSFRC and HSFRC) respectively, shown together with experimental results for SFRCs. On inspecting the numerical results for the load–CMOD diagrams of these three types of concrete beams under three-point bending, several features can be distinguished: (1) Load level I: the flexure stress increases linearly with deformation up to tensile strength of the materials, 5.2, 5.3, 5.4 MPa for plain concrete, HSFRC and SSFRC, respectively. In this stage, material behavior obeys elastic constitutive relationships and no fictitious crack is formed, therefore CMOD is equal to zero. (2) Load level II: the flexural stress increases up to 7.1, 9.0 and 9.1 MPa for plain concrete, HSFRC and SSFRC. In this period, the deformation increases little more than proportionally with respect to the stress. A fictitious crack develops in the middle of the beam and grows with the increasing load; (3) Load level III: the flexural stress increases up to the maximum values, the flexural modulus of the beam, about 10 MPa for these two FRCs. In this stage, the deformation increases much more than proportionally with respect to the stress. The difference on load–deformation behavior between HSFRC and SSFRC becomes distinct in stage

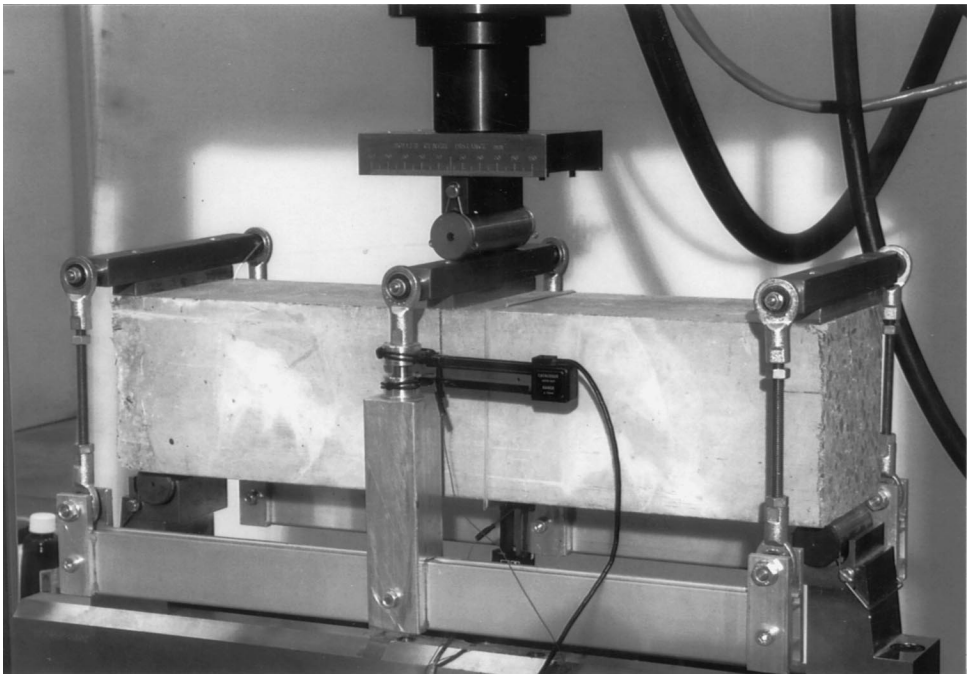

Fig. 9. Experimental setup used for FRC beams in three-point bending.

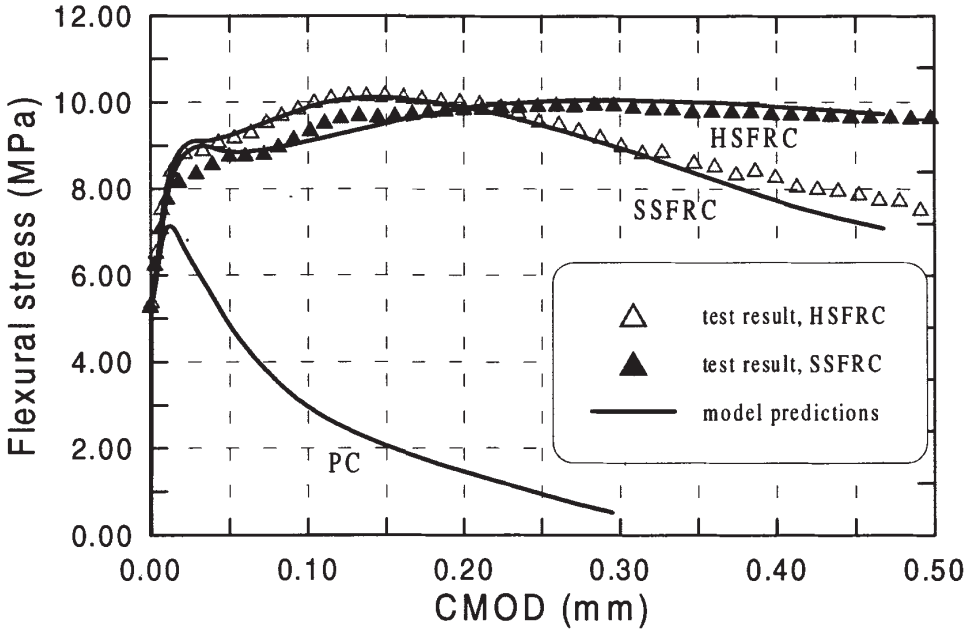

Fig. 10. Simulated flexure stress versus CMOD curves for plain concrete, SSFRC and HSFRC beams under three-point bending, shown together with experimental data.

III. This characteristic has also been found from experiments, i.e. the hooked fiber can improve the toughness more effectively than the straight fiber.

Fig. 11 shows the relationship between maximum flexural stress and fatigue life, the so-called S–N curves for these three types of concrete. Some experimental data are presented, together with the theoretical results. It can be seen that model prediction agrees well with the test results. First, the S–Log(N) curve of plain concrete is almost linear, which agrees with a number of experi-

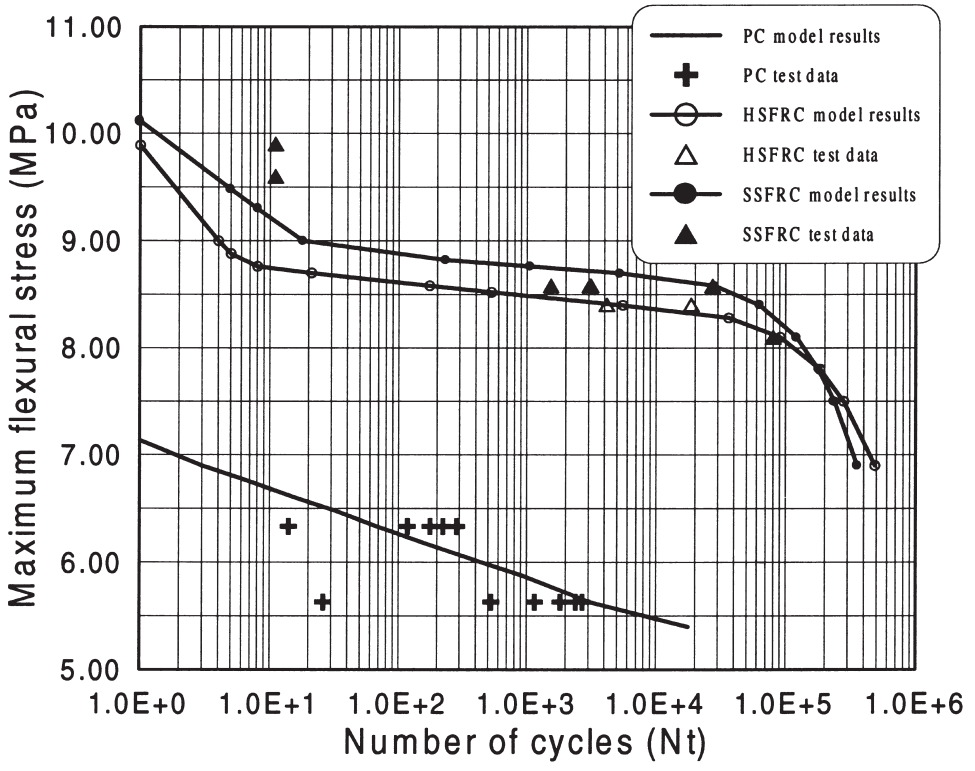

Fig. 11. Relationship of maximum flexure stress with fatigue life.

ments [6,23,24]. For steel fiber reinforced concrete the S–Log(N) curve becomes curved. Second, the present model predicts that the steel fibers can significantly improve the bending fatigue performance of concrete structures, which has been demonstrated by many researchers [1,3–6]. For steel fiber concrete beams, with maximum flexural stress between 9.00 and 10.00 MPa (level III), the fatigue life of SFRC is very short, within 1 to 30 cycles. The reason for this short fatigue life is a combination of a large initial crack length and significant bridging degradation due to large crack openings. With the maximum flexural stress between 5.3 or 5.4 and 9.00 MPa (level II), the fatigue life increases notably with the decreasing maximum flexural stress. The longer fatigue life is a product of both the shorter initial crack length and the smaller crack openings. When the maximum flexural stress is lower than 5.3 or 5.4 MPa (level I), no dominant macro fatigue crack occurs after the first cycle. However, fatigue crack initiation will not be addressed in the present paper.

4.3. Fatigue deformation characteristics

The numerical results for relationships between fatigue crack length and the number of cycles for three kinds of beam, plain concrete and two FRCs are shown in Fig. 12. The theoretical simulation successfully reproduced the three experimentally observed stages of crack growth [5], involving a decelerated stage, a steady state stage, and an accelerated stage towards final fracture failure. However, quantitatively the computed results and experimental data on CMOD do not compare well, see Fig. 13. One of the reasons is that the fatigue load can cause much more microcracking in the material than the monotonic load can. In fact, experimentally determined CMOD is not a single crack contribution within the gauge, 50 mm, length. Therefore, the measured CMOD is larger than the theoretical prediction due to microcracks next to the dominant crack within the gauge length under fatigue loading. This effect is more pronounced in the case of fiber reinforced concrete. If we introduce a factor, the so-called crack density factor, η, with η=1+0.4log(N), which describes the microcracking beside the main crack, that is a function of the number of cycles, good agreement between model predictions and experimental results, measured CMOD divided by η, can be found. It is shown in Fig. 13.

A general concept in the literature on concrete materials subjected to cyclic loading is that of an envelope curve, which provides a bound for the stress and strain (for compression) values that can be attained under general loading [2,24,25]. Most authors agree that this envelope either coincides with the monotonic loading curve, or is at least very close to this curve for plain concrete. This concept may be applicable for fatigue in compression, but is questionable for fatigue in flexure or tension. Based on the present investigation, bridging stress degradation exists in the fracture zone. This implies that the toughness of the beam gradually reduces with the number of cycles. Thus, it may be concluded that the CMOD and fatigue crack length as fatigue failure occurs will be less than the values that can be attained under the monotonic case for the same load level. Even further experimental verification is needed to support this conclusion. The difference between these two values is more obvious for fiber reinforced concrete than in the case of plain concrete. On the other hand, fatigue failure under bending or tension load will depend not only on the maximum load level, but also on the minimum load level, because they will affect the bridging degradation simultaneously. The theoretically calculated fatigue failure lines, in terms of fatigue crack length under different maximum load levels in the case of minimum load equal to zero for plain concrete and two types of FRC beams, are shown in Fig. 14. By comparing Fig. 14(a–c), it can be seen that fibers can normally increase the maximum fatigue crack length 15–20% of the depth of the beam, from 30 mm to 45–50 mm for plain concrete and FRC, respectively. This indicates that improved fatigue performance can be obtained by using fibers in concrete. From Fig. 14(b and c), we can see that the tendency of fatigue failure lines for SSFRC and HSFRC are different. The maximum fatigue crack length increases with lowering the maximum load level for SSFRC, while the opposite is the case for HSFRC. This can be explained from the cyclic bridging behavior of these two types of FRC materials. Due to the hook action, the bridging degradation is more notable in HSFRC than in SSFRC [12]. Therefore, the maximum fatigue crack length of HSFRC beams decreases with the decreasing maximum load.

4.4. Effect of minimum load level on fatigue life

Many experimental investigations have concluded that raising the minimum load can increase the fatigue life of concrete as well as FRCs [4,6,26]. But the mechanism of this effect has not been given much attention. Recent theoretical results have shown that raising the minimum load, i.e. increasing the minimum crack width, can reduce the crack bridging degradation, which in turn increases the fatigue life of FRCs [13]. On the other hand, if we assume that the fatigue crack also has a linear profile during unloading, then it can be deduced that the ratio between maximum and minimum crack widths at any crack location has the same value. Therefore, we can use the parameter φ in the cyclic crack bridging law to describe the effect of minimum load. Thus, in theory, we can predict the effect of the minimum load on the fatigue life.

Fig. 15 presents the model results of the effect of the parameter φ on the bending fatigue life of plain concrete

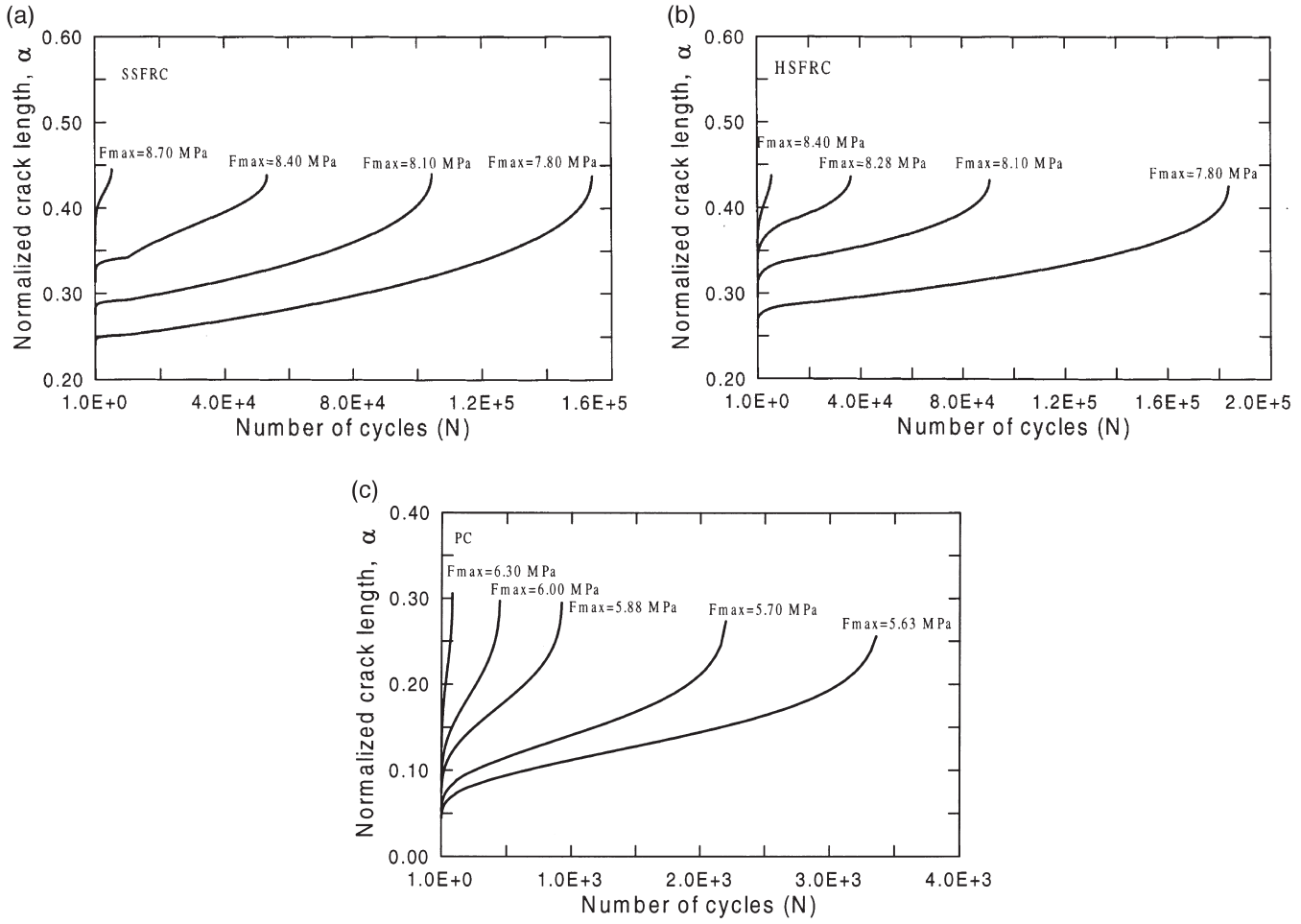

Fig. 12. Relationships of fatigue crack length and number of cycles. (a) SSFRC; (b) HSFRC and (c) PC.

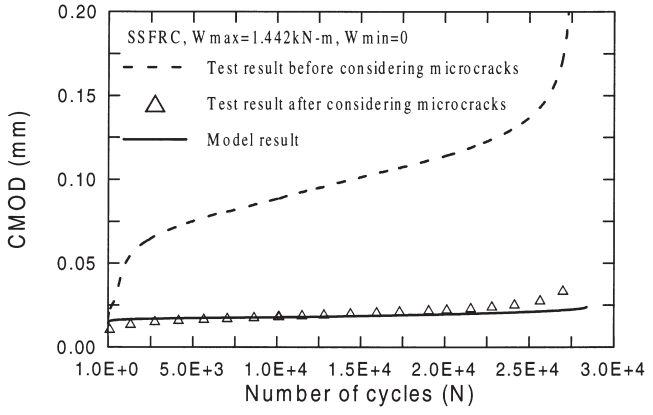

Fig. 13. Relationships of CMOD at maximum stress level and number of cycles, theoretical prediction and experimental result.

and FRC beams in terms of S–N diagrams. From these figures, we can see that the lower the value of φ, i.e. the higher the minimum loads, the longer the fatigue life. Fig. 16 gives some preliminary experimental results of the effect of the minimum load level ($R=M_{min}/M_{max}$) on the fatigue life of FRCs. Although the test data are very scattered, the tendency is quite clear. There is good agreement between theoretical predictions and experimental results, even although more detailed experimental investigation is needed to correlate the parameters φ and R except in the case of $\varphi=1.0\Leftrightarrow R=0$. This is due to the fact that the relationship between unloading load P and crack mouth opening δ can not be simply described by a linear relationship.

5. Conclusions

A semi-analytical approach for modelling the fatigue behavior in the flexure of plain concrete and FRC beams that relies on the cyclic stress–crack width relationship as the fundamental constitutive relationship in tension has been presented. The development of fatigue damage can be simulated through this model. Three cracking stages, which have been found in experiments, are represented through this model. The classical S–N curve is obtained and good correlation between the experiments and the model predictions is found.

The role and effectiveness of fibers in extending the

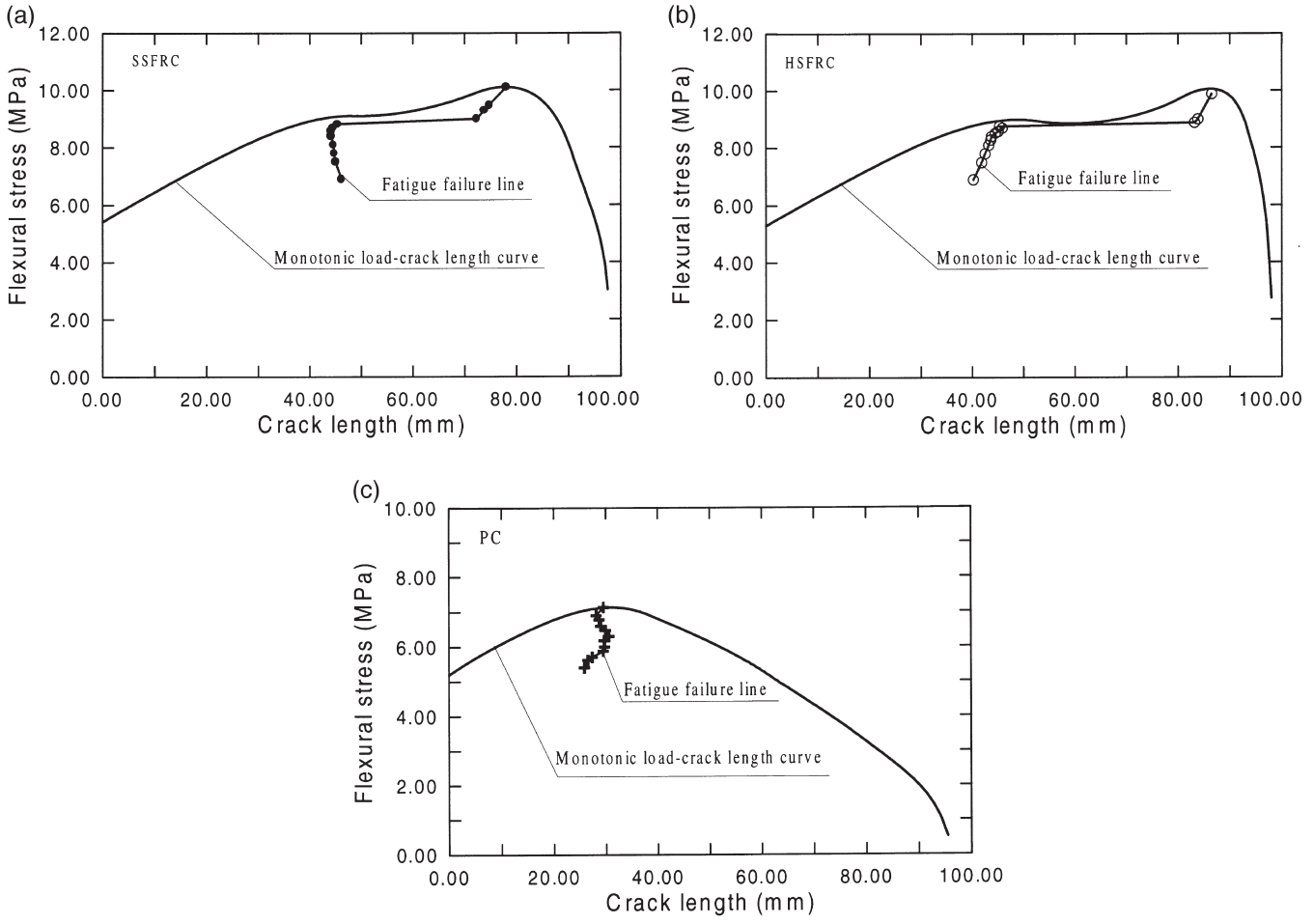

Fig. 14. Fatigue crack length at failure for different load levels. (a) SSFRC; (b) HSFRC and (c) PC.

fatigue life of concrete structures, which has been extensively demonstrated by many researchers, is successfully simulated with the present model. At the same time, this mechanism-based model has offered a theoretical foundation for understanding this phenomenon.

The general envelope curve concept that mainly is used for fatigue in the compression of plain concrete is inapplicable for fatigue in bending. Theoretical analysis shows that fatigue failure points under bending load do not coincide with the monotonic loading curve. Due to bridging degradation under cyclic loading, the failure strain, in terms of fatigue crack length or CMOD, will be less than the values that can be achieved under monotonic load with the same load level. The fatigue failure points under bending or tension load will depend on both the maximum and minimum loads, since both influence the bridging degradation. Further experimental work is needed to verify this conclusion.

The influence of minimum load on the bending fatigue life of concrete and FRC beams, which has been investigated by some researchers, is simulated by the present fatigue model through the introduction of a parameter, φ, which describes the influence of minimum crack width on the rate of crack bridging degradation. Reasonable agreement between model predictions and experimental results is obtained.

From this model it can be deduced that the flexural fatigue performance of plain concrete and FRC materials is strongly dependent on the cyclic bridging law of the materials. This cyclic bridging law, also called the cyclic stress–crack width relationship, can be treated as a fundamental constitutive relationship of materials as has the monotonic stress–crack width relationship. The optimum of fatigue performance in bending can be achieved through optimising the cyclic bridging behavior of materials, finally leading to the modification of the bond characteristics of aggregate–matrix and fiber–matrix interfaces, which is one of the principal sources of bridging degradation. The time-consuming fatigue tests can be replaced, or partly replaced, by uniaxial fatigue tensile tests on pre-cracked concrete and FRCs.

Acknowledgements

This work has been supported by a grant from the Danish Ministry of Education to the Technical Univer-

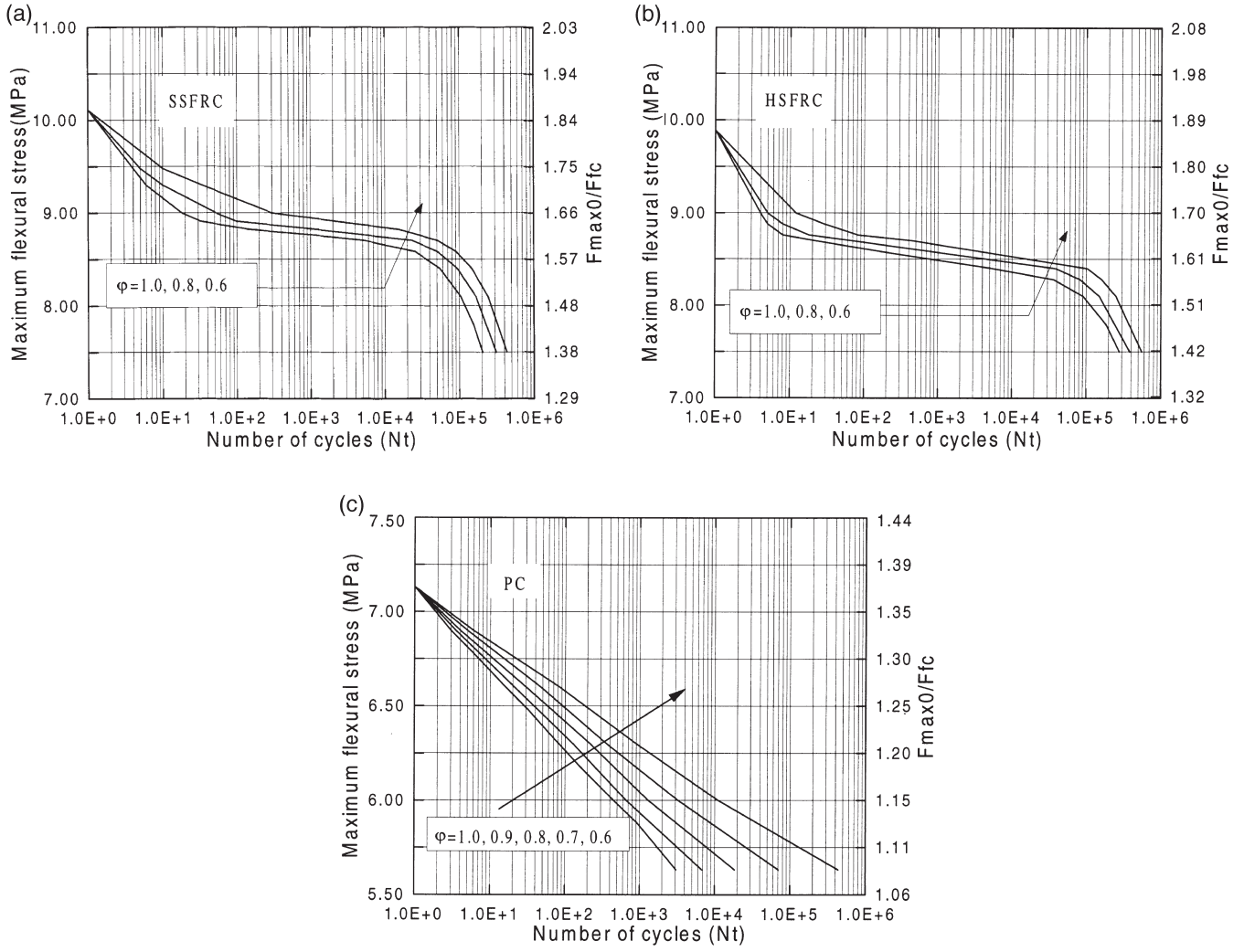

Fig. 15. Effect of minimum load (represented by parameter φ) on fatigue life, theoretical results.

sity of Denmark (DTU), and partly by a NATO grant, which supports collaboration research between the Department of Structural Engineering and Materials, DTU and the Advanced Civil Engineering Materials Research Laboratory, University of Michigan. Support from the National Science Foundation (CMS-9872357) to the University of Michigan is gratefully acknowledged.

Appendix A. Mathematical fit on cyclic crack bridging law of plain and steel fiber reinforced concrete

For straight steel fiber concrete (SSFRC), when one volume per cent straight steel fiber with circular cross-section, 0.4 mm in diameter and 25 mm in length, is used, the fitted cyclic bridging model is given by

$$\frac{\sigma_N}{\sigma_1} = \begin{cases} 1-\varphi k_1 \log(N) & (1 \le N \le 10) \\ 1-\varphi[(k_1-k_2)+k_2\log(N)] & (10 < N \le 10^4) \\ 1-\varphi[(k_1-k_2)+4(k_2-k_3)+k_3\log(N)] & (10^4 < N \le 10^5) \end{cases} \quad \text{(A1)}$$

where φ is the factor describing the influence of the minimum crack width, see Eq. (5). If the minimum crack width level corresponds to that at which the load is equal to zero during unloading, then φ is equal to one. The factors k_1, k_2, k_3 are all larger than zero and are functions of maximum crack width w_{max}. According to the test results carried out by Zhang et al. [12], they can be expressed as:

$$k_1 = \begin{cases} B_1 w_{max} & (0 \le w_{max} \le w_{01}) \\ (B_1-B_2)w_{01}+B_2 w_{max} & (w_{01} < w_{max} \le 0.5) \end{cases}$$

where B_1=1.43 mm^{-1}, B_2=−0.339 mm^{-1}, and w_{01}=0.166 mm.

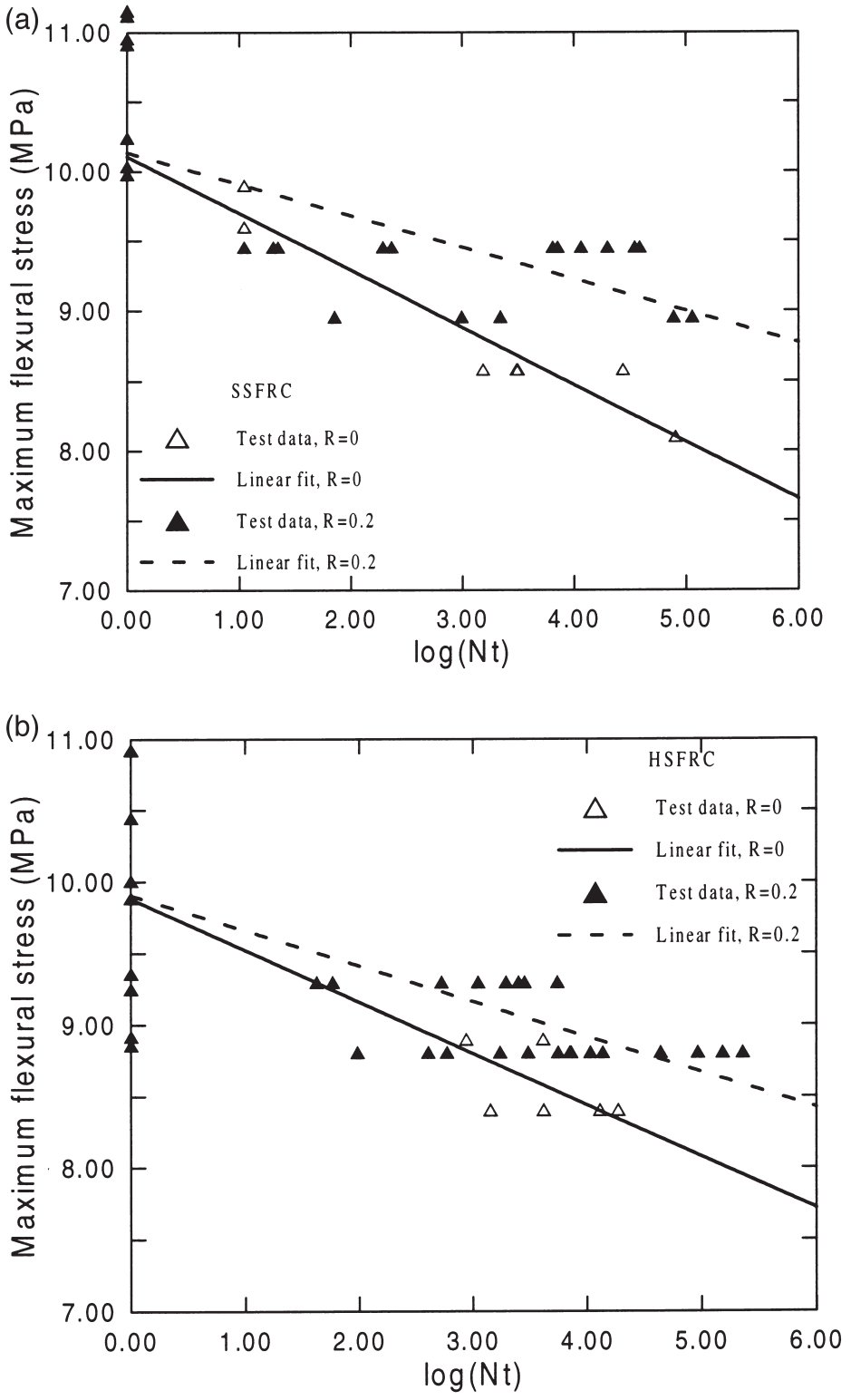

Fig. 16. Effect of minimum load on fatigue life, experimental results.

$$k_2=\begin{cases} C_1 w_{max} & (0\le w_{max}\le w_{02}) \\ (C_1-C_2)w_{01}+C_2 w_{max} & (w_{01}<w_{max}\le 0.5) \end{cases}$$

where C_1=0.9 mm^{-1}, C_2=−0.0982 mm^{-1}, and w_{02}=0.07 mm and

$$k_3=\begin{cases} D_1 w_{max}+A_3 & (0\le w_{max}\le w_{03}) \\ (D_1-D_2)w_{03}+A_3+D_2 w_{max} & (w_{03}<w_{max}\le 0.5) \end{cases}$$

where D_1=0.777 mm^{-1}, D_2=−0.0704 mm^{-1}, A_3=0.0432 and w_{03}=0.109 mm.

For hook-end steel fiber concrete (HSFRC), when one volume per cent hook-end steel fiber with a circular cross-section of 0.5 mm in diameter and 30 mm in length, is used, the similar cyclic bridging model is given by the following equations with φ identical to that given in Eq. (A1).

$$\frac{\sigma_N}{\sigma_1}=\begin{cases}1-\varphi k_1\log(N)\ (1\le N\le 10)\\ 1-\varphi[(k_1-k_2)+k_2\log(N)]\ (10<N\le 10^3)\\ 1-\varphi[(k_1-k_2)+3(k_2-k_3)+k_3\log(N)]\ (10^3<N\le 10^{3.5})\\ 1-\varphi[(k_1-k_2)+3(k_2-k_3)+3.5(k_3-k_4)+k_4\log(N)]\ (10^{3.5}<N\le 10^4)\\ 1-\varphi[(k_1-k_2)+3(k_2-k_3)+3.5(k_3-k_4)+4(k_4-k_5)+k_5\log(N)]\ (10^4<N\le 10^5)\end{cases} \quad \text{(A2)}$$

The factors k_1, k_2, k_3, k_4, k_5 are all larger than zero and functions of maximum crack width $w_{\max}$ as:

$$k_1=\begin{cases}B_1 w_{\max} & (0\le w_{\max}\le w_{01})\\ (B_1-B_2)w_{01}+B_2 w_{\max} & (w_{01}<w_{\max}\le 0.5)\end{cases}$$

where B_1=2 mm^{-1}, B_2=0.17 mm^{-1}, and w_{01}=0.088 mm.

$$k_2=\begin{cases}C_1 w_{\max} & (0\le w_{\max}\le w_{02})\\ (C_1-C_2)w_{01}+C_2 w_{\max} & (w_{01}<w_{\max}\le 0.5)\end{cases}$$

where C_1=1.2 mm^{-1}, C_2=−0.0982 mm^{-1}, and w_{02}=0.0613 mm and

$$k_3=\begin{cases}D_1 w_{\max}+A_3 & (0\le w_{\max}\le w_{03})\\ (D_1-D_2)w_{03}+A_3+D_2 w_{\max} & (w_{03}<w_{\max}\le 0.5)\end{cases}$$

where D_1=0.384 mm^{-1}, D_2=0, A_3=0.011.

$$k_4=\begin{cases}E_1 w_{\max}+A_4 & (0\le w_{\max}\le w_{04})\\ (E_1-E_2)w_{03}+A_4+E_2 w_{\max} & (w_{04}<w_{\max}\le 0.5)\end{cases}$$

where E_1=0.384 mm^{-1}, C_2=0.953 mm^{-1}, A_4=0.012 and w_{04}=0.0613 mm and

$$k_5=\begin{cases}F_1 w_{\max}+A_5 & (0\le w_{\max}\le w_{05})\\ (F_1-F_2)w_{05}+A_5+F_2 w_{\max} & (w_{05}<w_{\max}\le 0.5)\end{cases}$$

where F_1=1.7 mm^{-1}, F_2=−0.545 mm^{-1}, A_3=0.015 and w_{05}=0.225 mm.

For plain concrete, according to the investigation by Zhang et al. [12], the cyclic bridging law can be expressed as:

$$\frac{\sigma_N}{\sigma_1}=1-\varphi k\log(N) \quad \text{(A3)}$$

where k is given by:

$$k=\varphi(0.08+4w_{\max})$$

References

[1] Ramakrishan V, Oberling G, Tatnall P. Flexural fatigue strength of steel fibre reinforced concrete, SP-105. In: Detroit, Michigan: America Concrete Institute, 1987:225–45.

[2] Otter DE, Naaman AE. Properties of steel fibre reinforced concrete under cyclic loading. ACI Materials Journal 1988;85(4):254–61.

[3] Johnston CD, Zemp RW. Flexural performance of steel fiber reinforced concrete—influence of fibre content, aspect ratio and type. ACI Materials Journal 1991;88(4):374–83.

[4] Grzybowski M, Meyer C. Damage accumulation in concrete with and without fibre reinforcement. ACI Materials Journal 1993;90(6):594–604.

[5] Stang H, Zhang J. Experimental determination of fatigue crack growth in fibre reinforced concrete. In: Silva Gomez JF, et al., editors. Recent advances in experimental mechanics. 1994:1347–1352.

[6] Zhang J, Stang H. Fatigue performance in flexure of fibre reinforced concrete. ACI Materials Journal 1998;95(1):58–67.

[7] Li VC, Matsumoto T. Fatigue crack growth analysis of fibre reinforced concrete with effect of interfacial bond degradation. Cement and Concrete Composites 1998;20(5):353–63.

[8] Neville AM, Brooks JJ. Concrete technology. Longman Scientific and Technical, 1987.

[9] Zhang J, Stang H. Interfacial degradation in cement-based fibre reinforced composites. Journal of Materials Science Letters 1997;16(11):886–8.

[10] Matsumoto T. Fracture mechanics approach to fatigue life of discontinuous fibre reinforced composites. Doctoral Thesis, Department of Civil and Environmental Engineering, University of Michigan, 1998.

[11] Stang H, Aarre T. Evaluation of crack width in fibre reinforced concrete with conventional reinforcement. Cement and Concrete Composites 1992;14(2):143–54.

[12] Zhang J, Stang H, Li VC. Experimental study on bridging stress of fibre reinforced concrete under uniaxial fatigue tension. Accepted by ASCE Journal of Materials in Civil Engineering, 1998 (in press).

[13] Zhang J, Stang H, Li VC. Crack bridging model for fibre reinforced concrete under fatigue tension. Submitted for publication, 1998.

[14] Zhang J, Stang H. Application of stress crack width relationship in predicting the flexural behavior of fiber reinforced concrete. Cement and Concrete Research 1998;28(3):439–52.

[15] Hillerborg A, Modéer M, Petersson P-E. Analysis of crack formation and crack growth by means of fracture mechanics and finite elements. Cement and Concrete Research 1976;6:773–82.

[16] Ulfkjær JP, Krenk S, Brincker R. Analytical model for fictitious crack propagation in concrete beams. Journal of Engineering Mechanics 1995;121(1):7–14.

[17] Pedersen C. New production processes, materials and calculation techniques for fibre reinforced concrete pipes. PhD Thesis, Department of Structural Engineering and Materials, Technical University of Denmark, Series R, No. 14, 1996.

[18] Maalej M, Li VC. Flexural strength of fibre cementitious composites. Journal of Materials in Civil Engineering 1994;6(3):390–406.

[19] Maalej M, Li VC, Hashida T. Effect of fibre rupture on tensile properties of short fibre composites. Journal of Engineering Mechanics 1995;121(8):903–13.

[20] Li VC. Postcrack scaling relations for fibre reinforced cementitious composites. Journal of Materials in Civil Engineering 1992;4(1):41–57.

[21] Stang H. Application of the stress–crack width relationship in the design of FRC-structures. Department of Structural Engineering and Materials, Technical University of Denmark, 1997.

[22] Tada H. The stress analysis of cracks handbook. Paris: Paris Prod. Inc, 226 Woodbourn Dr., St. Louis, Missouri 63105, 1985.

[23] Holmen JO. Fatigue of concrete by constant and variable amplitude loading. Doctoral Thesis, NTH Trondheim, 1979.

[24] Kim J, Kim Y. Experimental study of the fatigue behaviour of

high strength concrete. Cement and Concrete Research 1996;26(10):1513–23.

[25] Byung B, Oh H. Fatigue analysis of plain concrete in flexure. Journal of Structural Engineering 1986;112(2):273–88.

[26] Zhang B, Phillips DV. Fatigue life of plain concrete under stress reversal. In: Shah SP, Swartz SE, Barr B, editors. Proceedings of the International Conference on Recent Developments in the Fracture of Concrete and Rock, 1989:183–92.